Simultaneous hyperspectral differential-CARS, TPF and SHG microscopy with a single 5 fs Ti:Sa laser

Iestyn Pope,[1] Wolfgang Langbein,[2] Peter Watson,[1] and Paola Borri[1,2,*]

[1] *Cardiff University School of Biosciences, Museum Avenue, Cardiff CF10 3AX, UK*
[2] *Cardiff University School of Physics and Astronomy, The Parade, Cardiff CF24 3AA, UK*
[*] *borrip@cardiff.ac.uk*

Abstract: We have developed a multimodal multiphoton laser-scanning microscope for cell imaging featuring simultaneous acquisition of differential Coherent Antistokes Raman Scattering (D-CARS), two-photon fluorescence (TPF) and second harmonic generation (SHG) using a single 5 fs Ti:Sa broadband (660-970 nm) laser. The spectral and temporal pulse requirements of these modalities were optimized independently by splitting the laser spectrum into three parts: TPF/SHG excitation ($>$ 900 nm), CARS Pump excitation ($<$ 730 nm), and CARS Stokes excitation (730-900 nm). In particular, by applying an equal linear chirp to pump and Stokes pulses using glass dispersion we achieved a CARS spectral resolution of 10 cm^{-1}, and acquired CARS images over the 1200-3800 cm^{-1} vibrational range selected by the time delay between pump and Stokes. A prism pulse compressor in the TPF/SHG excitation was used to achieve Fourier limited 30 fs pulses at the sample for optimum TPF and SHG. D-CARS was implemented with few passive optical elements and enabled simultaneous excitation and detection of two vibrational frequencies with a separation adjustable from 20 cm^{-1} to 150 cm^{-1} for selective chemical contrast and background suppression. The excitation/detection set-up using beam-scanning was built around a commercial inverted microscope stand providing conventional bright-field, differential interference contrast and epi-fluorescence for user-friendly characterization of biological samples. Examples of CARS hyperspectral images and simultaneous acquisition of D-CARS, TPF and SHG images in both forward and epi-direction are shown on HeLa cells, stem-cell derived human adipocytes and mouse tissues.

OCIS codes: (180.4315) Nonlinear Microscopy; (180.5655) Raman microscopy; (170.3880) Medical and biological imaging; (180.6900) Three-dimensional microscopy.

References and links

1. M. Muller and A. Zumbusch, "Coherent anti-stokes raman scattering microscopy," Chem. Phys. Chem. **8**, 2156–2170 (2007).
2. C. L. Evans and X. S. Xie, "Coherent anti-stokes raman scattering microscopy: Chemical imaging for biology and medicine," Annu. Rev. Anal. Chem. **1**, 883–909 (2008).
3. J. P. Pezacki, J. A. Blake, D. C. Danielson, D. C. Kennedy, R. K. Lyn, and R. Singaravelu, "Chemical contrast for imaging living systems: molecular vibrations drive cars microscopy," Nat. Chem. Biol. **7**, 137–145 (2011).
4. G. Krauss, T. Hanke, A. Sell, D. Träutlein, A. Leitenstorfer, R. Selm, M. Winterhalder, and A. Zumbusch, "Compact coherent anti-stokes raman scattering microscope based on a picosecond two-color er:fiber laser system," Opt. Lett. **34**, 2847–2849 (2009).

#181809 - $15.00 USD Received 14 Dec 2012; revised 1 Feb 2013; accepted 14 Feb 2013; published 13 Mar 2013

5. H. A. Rinia, M. Bonn, and M. Müller, "Quantitative multiplex cars spectroscopy in congested spectral regions," J. Phys. Chem. B **110**, 4472–4479 (2006).
6. R. Selm, M. Winterhalder, A. Zumbusch, G. Krauss, T. Hanke, A. Sell, and A. Leitenstorfer, "Ultrabroadband background-free coherent anti-stokes raman scattering microscopy based on a compact er:fiber laser system," Opt. Lett. **35**, 3282–3284 (2010).
7. B. von Vacano, L. Meyer, and M. Motzkus, "Rapid polymer blend imaging with quantitative broadband multiplex cars microscopy," J. Raman Spectrosc. **38**, 916–926 (2007).
8. Y. J. Lee, S. H. Parekh, Y. H. Kim, and M. T. Cicerone, "Optimized continuum from a photonic crystal fiber for broadband time-resolved coherent anti-stokes raman scattering," Opt. Express **18**, 4371–4379 (2010).
9. T. Hellerer, A. M. Enejder, and A. Zumbusch, "Spectral focusing: High spectral resolution spectroscopy with broad-bandwidth laser pulses," Appl. Phys. Lett. **85**, 25–27 (2004).
10. I. Rocha-Mendoza, W. Langbein, and P. Borri, "Coherent anti-stokes raman microspectroscopy using spectral focusing with glass dispersion," Appl. Phys. Lett. **93**, 201103 (2008).
11. W. Langbein, I. Rocha-Mendoza, and P. Borri, "Single source coherent anti-stokes raman microspectroscopy using spectral focusing," Appl. Phys. Lett. **95**, 081109 (2009).
12. B. Chen, J. Sung X Wu and S. Lim, "Chemical imaging and microspectroscopy with spectral focusing coherent anti-stokes raman scattering," J. of Biomed. Opt. **16**, 021112 (2011).
13. A. F. Pegoraro, A. Ridsdale, D. J. Moffatt, Y. Jia, J. P. Pezacki, and A. Stolow, "Optimally chirped multimodal cars microscopy based on a single ti:sapphire oscillator," Opt. Express **17**, 2984–2996 (2009).
14. I. Rocha-Mendoza, W. Langbein, P. Watson, and P. Borri, "Differential coherent anti-stokes raman scattering microscopy with linearly-chirped femtosecond laser pulses," Opt. Lett. **34**, 2258–2260 (2009).
15. I. Rocha-Mendoza, W. Langbein, and P. Borri, "Quadruplex cars micro-spectroscopy," J. Raman Spectrosc. **44**, 255-261(2013).
16. D. T. Shima, K. Haldar, R. Pepperkok, R. Watson, and G. Warren, "Partitioning of the golgi apparatus during mitosis in living hela cells," J. Cell Biol. **137**, 1211-1228 (1997).
17. C. D. Napoli, F. Masia, I. Pope, C. Otto, W. Langbein, and P. Borri, "Chemically-specific dual/differential cars micro-spectroscopy of saturated and unsaturated lipid droplets," J. Biophotonics (2012), published online DOI 10.1002/jbio.201200197.

1. Introduction

Coherent anti-Stokes Raman scattering (CARS) microscopy has emerged in the last decade as a powerful tool for cell biologists to examine living cells with chemical specificity and three-dimensional (3D) spatial resolution in a label-free, non-invasive way [1–3]. CARS is a third-order nonlinear process (four-wave mixing) where molecular vibrations are coherently driven by the interference between two optical fields (pump and Stokes) and a third field (the pump itself in a two-pulse CARS system) is used to generate anti-Stokes Raman scattering from the driven vibrations. Owing to the coherence of the driving process, CARS benefits, unlike spontaneous Raman, from the constructive interference of light scattered by spectrally overlapping vibrational modes within the focal volume, thus enabling fast acquisition at moderate powers compatible with live cell imaging. Its nonlinear nature also implies that CARS is generated only in the focal volume where high photon densities are reached, allowing for an intrinsic 3D spatial resolution (optical sectioning) similar to other multiphoton microscopy techniques such as two photon fluorescence (TPF) and second harmonic generation (SHG).

Since typical vibrational resonances in liquid have coherence times in the picosecond range, CARS is preferably implemented with picosecond lasers [2]. However these systems tend to be expensive and non trivial to operate. It was recently shown that picosecond Er:fiber lasers can be used as a compact cost-effective source for CARS, however they offer limited output powers [4]. Furthermore picosecond pulses are inefficient at exciting TPF and SHG thus do not lend themselves to multimodal imaging systems. For these reasons CARS systems based on femtosecond lasers have attracted increasing attention. To achieve high spectral resolution in CARS with femtosecond laser sources different approaches have been considered. On the one hand, the broadband spectrum of femtosecond pulses can be used to excite several vibrational frequencies simultaneously while narrow spectral resolution is maintained with a narrow-band picosecond pulse acting as probe. This has been shown with femtosecond and picosecond syn-

#181809 - $15.00 USD Received 14 Dec 2012; revised 1 Feb 2013; accepted 14 Feb 2013; published 13 Mar 2013

chronized Ti:Sa laser sources, which are expensive and complicated [5], or with fiber-based systems (doped-fiber lasers [6] or continuum generation in photonic crystal fibers - PCF [7,8]) which are more compact and cost-effective but suffer from limited output powers. Moreover, doped-fiber lasers generate wavelengths > 1100 nm which necessitate microscope objectives well corrected in the infrared range, that are usually very expensive. Another way to use femtosecond pulses and maintain high-spectral resolution is by controlling the spectral selectivity in the excitation through phase shaping. This enables the use of a single broadband femtosecond source and fast and efficient single-channel detectors in contrast to spectrally-resolved multiplexing techniques. A straightforward and efficient way to perform phase shaping termed "spectral focusing" is achieved by applying an equal linear chirp to pump and Stokes pulses, hence creating a constant instantaneous frequency difference (IFD) between them which selectively drives a vibrational excitation of interest [9–11]. The spectral resolution is given by the Fourier-limit of the temporal envelop of the chirped pulses which can be elongated to a few picoseconds. This implementation was recently shown by us and other groups using a single broadband source in the form of a sub-10fs Ti:Sa oscillator [11,12] or a PCF pumped by a 100 fs Ti:Sa laser [12,13]. A major advantage of sub-10fs Ti:Sa lasers over PCFs is their larger output power and their stable and flat spectral phase. In our previous work, we used a 8 fs Ti:Sa laser and demonstrated spectral focusing with simple passive optical elements [11]. We created a vibrational excitation tuneable over the spectral range of 800-2200 cm^{-1} with an adjustable spectral resolution in the 10-100cm^{-1} range. We also showed dual-frequency differential-CARS (D-CARS) as a simple and efficient way to reject nonresonant CARS background and improve the chemical selectivity by simultaneously exciting two vibrational resonances and measuring the difference in the corresponding CARS intensities [11, 14, 15].

In this paper, we describe our second generation single-broadband-laser CARS microscope featuring spectral focusing and simultaneous dual-frequency acquisition using a 5 fs Ti:Sa source with 310 nm bandwidth hence capable of exciting a much wider vibrational range from 1200 cm^{-1} to 3800 cm^{-1} compared to our previous work [11]. This range covers biologically relevant frequencies from the fingerprint region to the high frequency C-H stretching vibrations commonly used for imaging lipids in living cells [2]. Furthermore, the large bandwidth of the laser spectrum enabled us to use a part for efficient two-photon excitation (TPE) of TPF and SHG simultaneously with CARS. Compared to our first generation fully home-built CARS microscope [10, 11, 14, 15], the excitation/detection is coupled with an inverted commercial microscope offering conventional epi-fluorescence and differential interference contrast (DIC) and equipped with a temperature-stabilised environmental chamber and CO_2 supply, for user-friendly studies on living cells.

2. Experimental set-up

2.1. Excitation beam preparation

A schematic of the experimental setup is shown in Fig. 1. We use a single Ti:sapphire laser source (Venteon, Pulse:One PE) to simultaneously provide both CARS and TPF/SHG excitation. The Ti:sapphire laser is pumped by a Nd:vanadate laser (Laser Quantum, Finesse) at 5.5 W and generates 5 fs pulses with a spectral width of 310 nm at 10% of the maximum intensity (660 nm to 970 nm, see inset of Fig. 1) at a repetition rate of 80 MHz with a time-average output power of 600 mW. The laser power is controlled by an achromatic half-wave plate and a Glan-laser polariser. The plate rotation is computer-controlled providing a calibrated transmission range from 1 to 10^{-2}. A long-pass filter (two 3 mm thick RG645 in Brewster angle) is used to reject the tail of the laser spectrum in overlap with the CARS detection range. The pulse spectrum is then split into three components providing the pump, Stokes and TPE. Firstly a custom short-pass dichroic mirror (Eksma Optics, DM1a in Fig. 1) is reflecting wavelengths

#181809 - $15.00 USD Received 14 Dec 2012; revised 1 Feb 2013; accepted 14 Feb 2013; published 13 Mar 2013

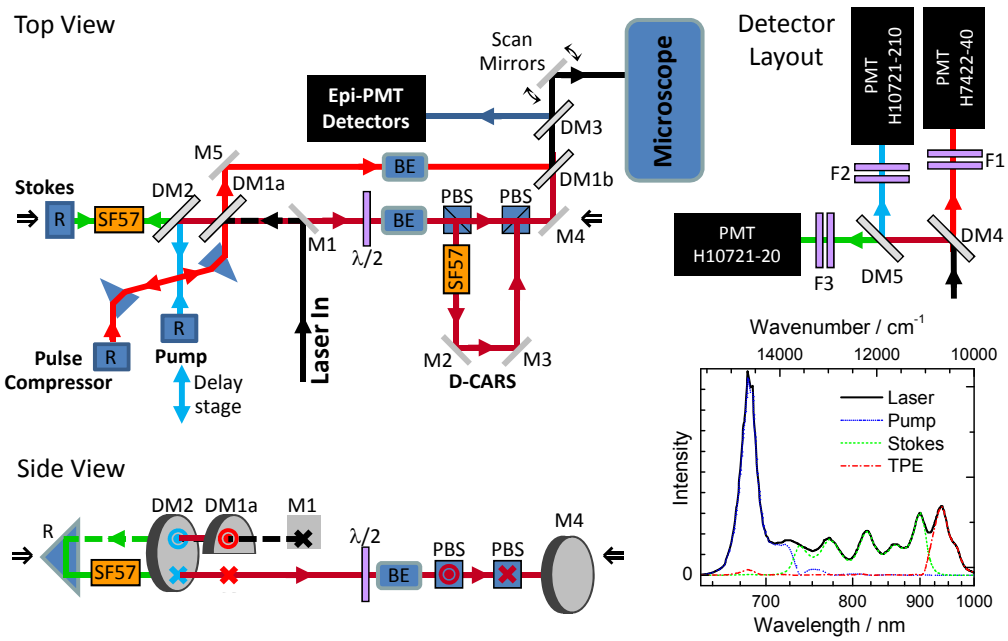

Fig. 1. Sketch of the microscope set-up. M: mirror; DM: dichroic mirror; SF57: glass blocks; R: reflecting prism; $\lambda/2$: half-wave plate; BE: beam expander; PBS: polarizing beam splitter; F: filter. The side view of the optics between by the two indicated arrows shows the beam height difference. Graph: typical spectra of the laser, pump, Stokes and TPE beams.

$>$ 900 nm for the TPF/SHG excitation beam. The resulting pulse is centred at 940 nm with a bandwidth of 70 nm (at 10% of the peak). The transmitted beam is separated into pump and Stokes by a second dichroic mirror (CVI Melles Griot, LWP-450RP670-TP830-PW-1025-C, DM2 in Fig. 1). The resulting pump and Stokes pulses are centred at 682 nm (14,663 cm^{-1}) and 806 nm (12,400 cm^{-1}), with a bandwidth at 10% of 65 nm and 200 nm respectively. DM1a as well as the coupling mirror M1 are half cut, as sketched in Fig. 1. In this way, pump and Stokes beams after traveling through vertically displacing prism reflectors (R) are recombined by DM2 at a lower height and transmitted below DM1a.

In TPE the two-photon resonances are either driven off-resonantly as typically in SHG, or have a wide spectral bandwidth of the two-photon absorption cross-section in TPF. Therefore, for a given pulse energy TPE scales inversely with the pulse duration down to the 10 fs range, such that efficient TPE is achieved for a Fourier-limited pulse at the sample which requires to compensate the group-delay dispersion (GDD) of the microscope optics. The GDD at the wavelength of the TPE in our set-up (940 nm) is sufficiently small to use a prism-based compressor as shown in Fig. 1 which consists of two SF58 prisms (Fortune Optronics) with 50 mm distance, resulting in Fourier-limited pulses of approximately 30 fs duration at the sample.

Conversely, vibrational resonances in liquids have coherence times in the picosecond range, therefore their coherent excitation in the CARS process is optimized in spectral selectivity using picosecond pulses. Since the vibrational excitation is governed by the interference between pump and Stokes field, it is possible to use femtosecond pulses and still achieve a high spectral resolution by spectral focussing [9]. We have demonstrated that this can be achieved simply and efficiently using glass elements of known group velocity dispersion [10, 11, 14]. Similar to our previous works, we have used SF57 glass blocks of variable length for this purpose. The Stokes

#181809 - $15.00 USD Received 14 Dec 2012; revised 1 Feb 2013; accepted 14 Feb 2013; published 13 Mar 2013

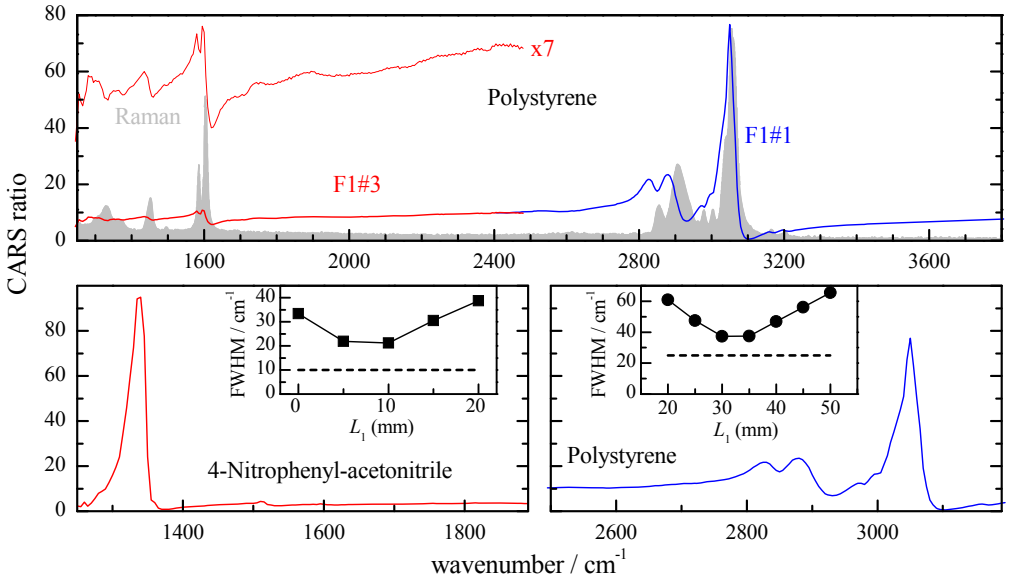

Fig. 2. Top: Spectrum of the CARS intensity ratio of polystyrene relative to glass (solid line) and spontaneous Raman (grey area, taken from http://www.sigmaaldrich.com/). F1#1 (F1#3) are the detection filters (see Table 1) used below (above) 2450cm^{-1}, respectively. Bottom: CARS ratio of 4-Nitrophenylacetonitrile (left) and polystyrene (right), with insets showing the CARS linewidths (full width at half maximum) of the 1340cm^{-1} (left) and 3054cm^{-1} (right) resonance as a function of the Stokes glass length L_1. Dashed lines in the insets indicate the Raman linewidths.

beam travels through a glass block of length L_1 which can be adjusted from 0 mm to 60 mm in steps of 5 mm by using blocks of different length mounted on two computer-controlled holders for automated exchange. GDD is further accrued by both pump and Stokes up to the sample from their propagation through the scan lens, the tube lens and the microscope objective. At 680 nm this GDD was found to be around 15200(16000) fs^2, for the 20×(60×) objective, respectively (see section 2.2). The key point of spectral focussing is to linearly chirp both pulses with the same chirp parameter (called β in Ref. [10]) proportional to the GDD. Hence, the extra length L_1 in the Stokes pulse is needed because the GDD for normal dispersion is smaller at the Stokes wavelength compared to the pump. The chirp of the Stokes can be adjusted by varying L_1 to match that of the pump, optimizing the spectral resolution. By measuring the CARS linewidth as a function of L_1 for the aromatic CH vibration of polystyrene at 3054 cm^{-1} and for the vibration of 4-Nitrophenylacetonitrile at 1340 cm^{-1} we found an optimum resolution of about 10 cm^{-1} (see Fig. 2), consistent with the chirped pump pulse duration of about 1 ps at the sample. Noticeably, the matching length L_1 is significantly higher at 3050 cm^{-1} ($L_1 = 30$ mm) compared to 1340 cm^{-1} ($L_1 = 10$ mm). This is due to non-linear chirp affecting the broadband Stokes pulse which can be approximated as linear only for a limited wavelength range and thus requires different lengths L_1 to match the pump chirp at different Stokes center wavelengths. The relative delay time between pump and Stokes is controlled with 5 fs precision via a delay stage (PI, M-404.42S) on the pump beam path. Tuning this delay shifts the instantaneous frequency difference (IFD) between the equally linearly chirped pump and Stokes and enables us to perform CARS spectroscopy rapidly without adjustments to the laser [10].

To implement D-CARS [14] the pump-Stokes pair is split into two orthogonally polarised pairs Π_1 and Π_2 using a computer-controlled half-wave plate and a polarising beam splitter

#181809 - $15.00 USD Received 14 Dec 2012; revised 1 Feb 2013; accepted 14 Feb 2013; published 13 Mar 2013

Table 1. Filters in forward and epi detection, from Semrock or †CVI Melles Griot.

Detection	Position in Fig. 1	Filters	Transmission range	Signal
Forward	F1#1	FF01-562/40 ×2	542–582 nm 3790–2520 cm^{-1}	CARS
Forward	F1#2	FF01-593/40 ×2	573–613 nm 2790–1650 cm^{-1}	CARS
Forward	F1#3	SP01-633RS FF01-609/54 †FSWP-750	582–630 nm 2520–1210 cm^{-1}	CARS
Forward	F2	FF01-510/84 FF01-469/35	468–487 nm	SHG
Forward	F3	FF01-510/84 ×2	468–552 nm	TPF
Epi	F1	FF01-562/40 ×2	542–582 nm 3790–2520 cm^{-1}	CARS
Epi	F2	FF01-510/84 FF01-475/50	468–500 nm	SHG
Epi	F3	FF01-510/84 ×2	468–552 nm	TPF

(PBS). The second pair Π_2 travels over an additional path providing a delay equal to half the laser repetition period and is recombined with Π_1 by a second PBS. By frequency analyzing the correspondingly periodic CARS signal, we can simultaneously detect the dc component proportional to the sum of the CARS signal from Π_1 and Π_2 and the ac component at the pulse repetition rate proportional to the difference of the CARS signal from Π_1 and Π_2. Via the insertion of thin (few mm) SF57 glass element in the beam path of Π_2 we can delay the pump and Stokes pulses as a result of their different group velocity and in turn change the IFD of Π_2. Consequently, we can detect simultaneously the sum and difference of the CARS intensity at two IFDs which can be chosen to coincide with characteristic frequencies in the CARS response of a material and in turn improve the chemical specificity of the technique. Moreover when the difference between the IFDs (Δ_{IFD}) in the D-CARS is sufficiently small, the D-CARS spectrum resembles the first derivative of the CARS spectrum and recovers a lineshape similar to that of spontaneous Raman if the resonant CARS is weak compared to the non-resonant background [11]. In practice in this set-up, Δ_{IFD} was adjustable from 20 cm^{-1} to 150 cm^{-1}.

Pump, Stokes and TPE beams are recombined using a dichroic mirror (DM1b, spectral characteristics as DM1a) prior to entering the scan mirrors (Cambridge Technology, 6210HSM40). A scan lens (from a Nikon A1RMP multiphoton microscope) is used to focus the collimated beam from the scan mirrors into the intermediate image plane at the microscope port, and is imaging the scan mirrors into the back focal plane of the microscope objective to reduce vignetting during scanning. Galilean beam expanders in the pump/Stokes and TPE are used to adjust the beam size to fill the back-aperture of the objective.

2.2. The inverted microscope

The excitation beams enter a Nikon Ti-U inverted microscope through the left port. The microscope is equipped with a selection of objectives and condensers. For a large field-of-view, we use a 20× 0.75 NA dry objective (Nikon CFI Plan Apochromat λ series) and a 0.72 NA dry condenser with a differential interference contrast (DIC) module. For high resolution we use a 60× 1.27 NA water immersion objective (Nikon CFI Plan Apochromat IR λS series)

#181809 - $15.00 USD Received 14 Dec 2012; revised 1 Feb 2013; accepted 14 Feb 2013; published 13 Mar 2013

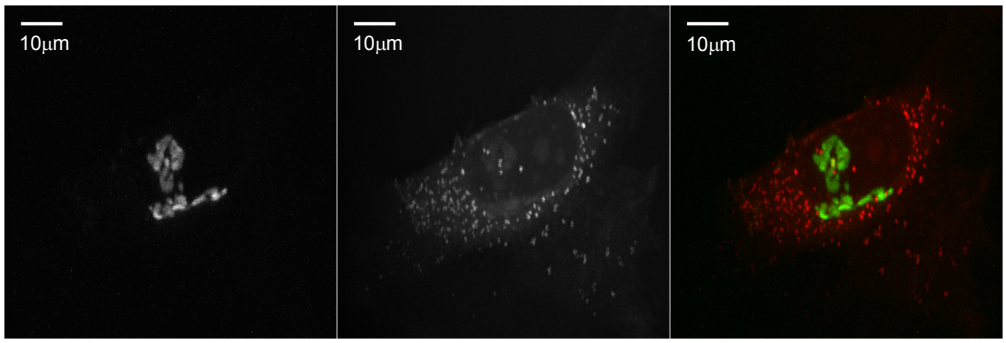

Fig. 3. Simultaneously acquired epi-TPF (left), and forward CARS (middle) images (on a linear grey scale) of live Hela cells transfected with a GFP-Golgi label using the 60× 1.27 NA objective. Images cover a *xyz* range of 80 μm×80 μm×10 μm with 800×800×50 pixels, and are shown as maximum intensity projections along *z*. CARS was acquired with only Π_1 at 2850 cm^{-1}. Excitation powers at the sample were TPE 6 mW, Pump 27 mW, and Stokes 13 mW. The false color image (right) overlays the CARS (red) and TPF (green) images. Pixel dwell time = 0.01 ms; 6.4 seconds per *xy* image.

and a 1.4 NA oil condenser with both a DIC and a (home-built) dark-field module. We measured a CARS spatial resolution (full-width at half-maximum of the intensity point-spread function) with the 0.75 NA objective of 0.6 (1.1) μm in the lateral (axial) direction, and with the 1.27 NA objective of 0.3 (0.44) μm in the lateral(axial) direction. The condenser is used both for brightfield/darkfield/DIC imaging and to collect the forward emission generated by CARS and TPF/SHG. XY sample motion and Z-objective motion is automated by stepper motors (Prior ProScan III). A metal-halide light source (Prior Lumen 200) provides epi-fluorescence illumination. Transmission and epi-fluorescence images are acquired by a monochrome CCD camera (Hamamatsu Orca-285) mounted on the right port.

2.3. CARS, TPF and SHG detection

CARS, TPF and SHG emission are collected in both forward and epi directions. To enable forward detection, the illumination pillar of the Nikon Ti-U microscope was modified to allow computer controlled removal of the 90 degree mirror reflecting the halogen transillumination towards the condenser. The signal collected by the condenser lens is projected upwards into a cluster of three photo multipliers tubes (PMTs) mounted on top of the illumination pillar, with a layout shown in Fig. 1. A dichroic beamsplitter (Semrock FF520-Di02, DM4 in Fig. 1) transmits the CARS emission at $>$ 540 nm and reflects the shorter wavelength TPF and SHG signals. In the CARS signal path, two computer controlled filter wheels provide a selection of bandpass filters (Table 1), rejecting pump and Stokes and transmitting CARS over appropriate spectral bands. CARS is detected by a Hamamatsu H7422-40 PMT with 38% quantum efficiency (QE) at 560 nm. The signal reflected by DM4 is separated into SHG and TPF by a second dichroic mirror (Chroma t495lp, DM5 in Fig. 1) and appropriate bandpass filters (see Table 1). The SHG (TPF) is detected by a Hamamatsu H107210-210 (H10721-20) PMT with 30% (18%) QE at 470(510) nm, respectively. The epi-detected signal is collected by the microscope objective, travels backwards along the excitation path over the scan mirrors, and is reflected by a dichroic mirror (Semrock FF660-Di02, DM3 in Fig. 1) into a cluster of three PMTs similar to the forward cluster, with filters as given in Table 1. In both forward / epi detection, the back focal plane of the condenser / objective is imaged onto the PMT cathodes with a matching size by appropriate lenses.

#181809 - $15.00 USD Received 14 Dec 2012; revised 1 Feb 2013; accepted 14 Feb 2013; published 13 Mar 2013

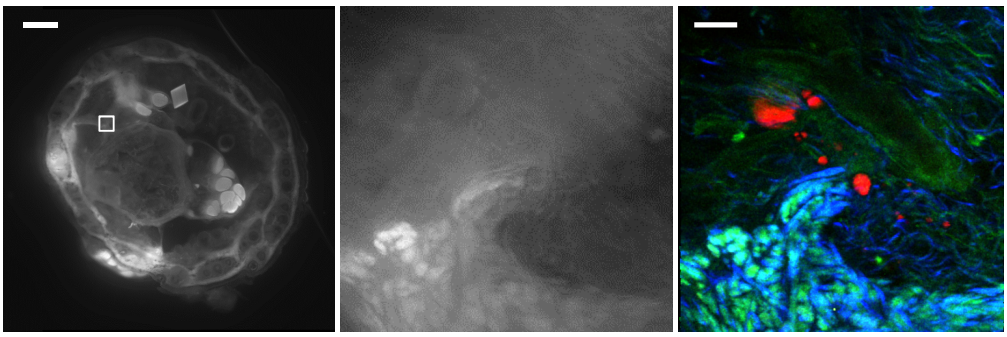

Fig. 4. Mouse tail tissue section fluorescently labeled with FITC-Concanavalin A. Left: Stitched epi-fluorescence image, scale bar = 300 μm. Middle: Single epi-fluorecence image cropped to 150×150 μm of the boxed region shown on the left. Right: False colour TPF (green), CARS from subcutaneous lipid deposits at 2850 cm^{-1} (red) and SHG from collagen (blue), scale bar = 20 μm. Excitation powers at the sample were TPE 7 mW, Pump 14 mW, and Stokes 7 mW. 20$\times$ 0.75 NA objective. 150×150 μm, 501×501 pixels, 0.01 ms pixel dwell time (2.5 s total image acquisition).

3. Simultaneous D-CARS/CARS, TPF and SHG imaging

To demonstrate the multimodal capabilities and high spatial and spectral resolution of the microscope we show in the following exemplar images on live Hela cells, fixed stem cell derived human adipocytes, and a mouse tail tissue section.

Simultaneous CARS and TPF acquisition with high 3D spatial resolution on live Hela cells is shown in Fig. 3. HeLa (A.T.C.C. CCL-2) cells were grown on 25 mm-diameter coverslips in DMEM (Dulbeccos modified Eagles medium; Life Technologies) medium supplemented with 10% (v/v) FCS (foetal calf serum) and 1% L-glutamine. Cells were transfected with the EGFP-tagged marker of the Golgi apparatus NAGFP (EGFP fused to the Golgi retention signal of N-acetylglucosaminyltransferase I) [16]. To induce the formation of lipid droplets, growth media was supplemented for three hours prior to imaging with 20 μg/ml oleic acid (Fatty acid/albumin complex O3008, Sigma). Coverslips containing HeLa cells were mounted in an imaging chamber equivalent to a 35 mm dish and placed in the microscope environmental chamber and maintained at 37°C in a humidified 5% CO_2 atmosphere. Simultaneously acquired epi-TFP and forward-CARS *xyz* images were generated using the 60$\times$ 1.27 NA objective and 0.72 NA condenser lens. CARS was acquired using pair Π_1 exciting the 2850 cm^{-1} CH_2 symmetric stretch resonance abundant in the acyl chain of fatty acids. The Golgi structure adjacent to the cell nucleus is clearly visible in the TPF, while small cytosolic lipid droplets are visible in CARS and their 3D movement manifests as stripe-like shapes in the 2D projection. Note that cells survived under the indicated raster scanning conditions with acquisitions repeated every 5 min on average for over 2 hours without any noticeable damage.

A complete set of CARS, TPF and SHG images simultaneously acquired in forward and epi detection are shown in Fig. 4 and Fig. 5. Images were taken on a c57bl6 mouse tail section stained with fluorescein isothiocyanate (FITC) labeled Concanavalin A, which is a generic cell marker binding glycosylated proteins and lipids. FITC has excitation and emission spectrum peak wavelengths at 495 nm and 521 nm respectively, matching the TPE and TPF detection wavelengths. The tissue section was sandwiched between a coverslip and a glass slide using 120 μm thick imaging gaskets filled with water (note that the IFD shifts by less than 1 cm^{-1} over the 120 μm sample thickness, which is negligible compared to the IFD resolution). Images were taken with the 20$\times$ 0.75 NA objective and the 0.72 NA condenser. CARS was acquired

#181809 - $15.00 USD Received 14 Dec 2012; revised 1 Feb 2013; accepted 14 Feb 2013; published 13 Mar 2013

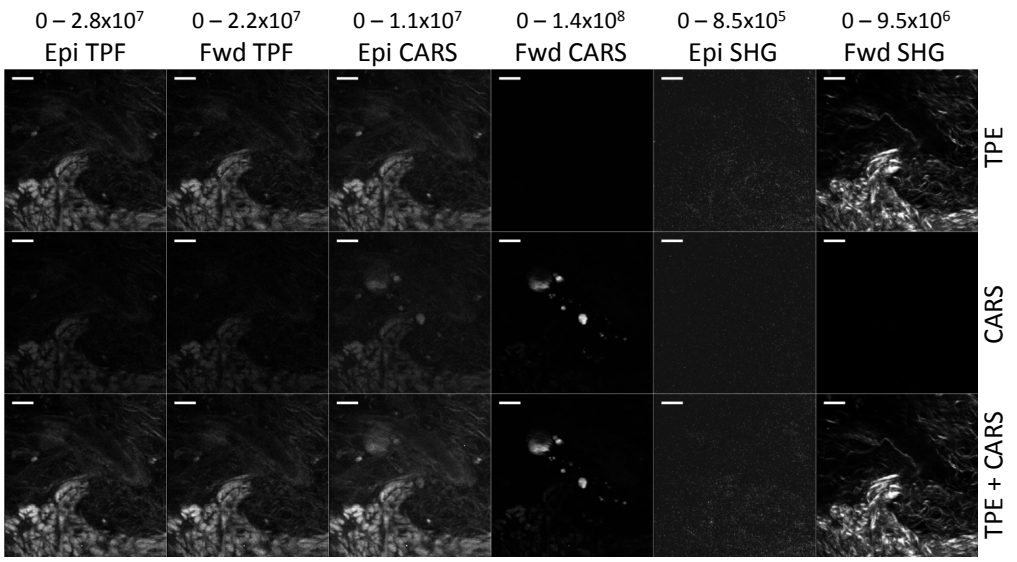

Fig. 5. Simultaneously acquired images for TPE (top row), pump and Stokes excitation at 2850 cm^{-1} (middle row), and CARS with TPE (bottom row) of the mouse tail section in Fig. 4. Linear grey scale over the range shown at the top of each column in photoelectrons/sec at the PMT cathode. Scale bar 20 μm.

using pair Π_1 exciting the 2850 cm^{-1} CH_2 and shows subcutaneous lipid deposits, while SHG shows the extracellular collagen matrix in the tissue.

To further elucidate the specificity and multimodality of our excitation and detection scheme, we show in Fig. 5 all images simultaneously detected by the six PMTs for TPE (top), pump and Stokes excitation (middle), and TPE with pump and Stokes (bottom). Using TPE only, no CARS signal is generated, but some fluorescence is detected by the CARS PMTs, due to the spectral tail of the FITC which extends into the CARS detection region > 540 nm (see Table 1). However this signal is more than one order of magnitude lower than the CARS signal and thus negligible when plotted on the same scale as the CARS image (see forward CARS column in Fig. 5). Using pump and Stokes excitation only, weak TPF and negligible SHG is observed. Furthermore only weak epi-detected SHG is measured, as expected from the directionality of coherent SHG emission.

CARS and D-CARS hyperspectral imaging is demonstrated in Fig. 6. Human adipose derived stem cells were obtained from Invitrogen (R7788-110) and cultured in DMEM (low glucose) containing Glutamax supplemented with 10% Mesenchymal stem cell qualified FBS, 75 μg/mL Gentamicin and 37.5 ng/mL Amphotericin. For adipogenic differentiation ADSCs were grown in complete StemPro adipogenic differentiation media (Invitrogen) according to the manufacturers instructions. After fixation, coverslips with cells were mounted onto standard glass slides using 120 μm thick imaging gaskets filled with water, and images were taken with the 60$\times$ 1.27 NA objective and 0.72 NA condenser lens. Stacks of *xy* images were taken for a series of IFDs covering both the fingerprint and the CH-stretch vibrational range. Examples of CARS and D-CARS spectra of a specific lipid droplet, and corresponding extracts of *xy* images at specific IFDs are shown (*xy*-IFD hyperspectral movies Media 1 and Media 2 are given as hyperlinks in the caption). D-CARS offers improved chemical specificity by discriminating spectral variations from spatial variations of the CARS intensity, as shown in our earlier works on polystyrene and PMMA beads [11, 14]. More recently, we have demonstrated the ability

#181809 - $15.00 USD Received 14 Dec 2012; revised 1 Feb 2013; accepted 14 Feb 2013; published 13 Mar 2013

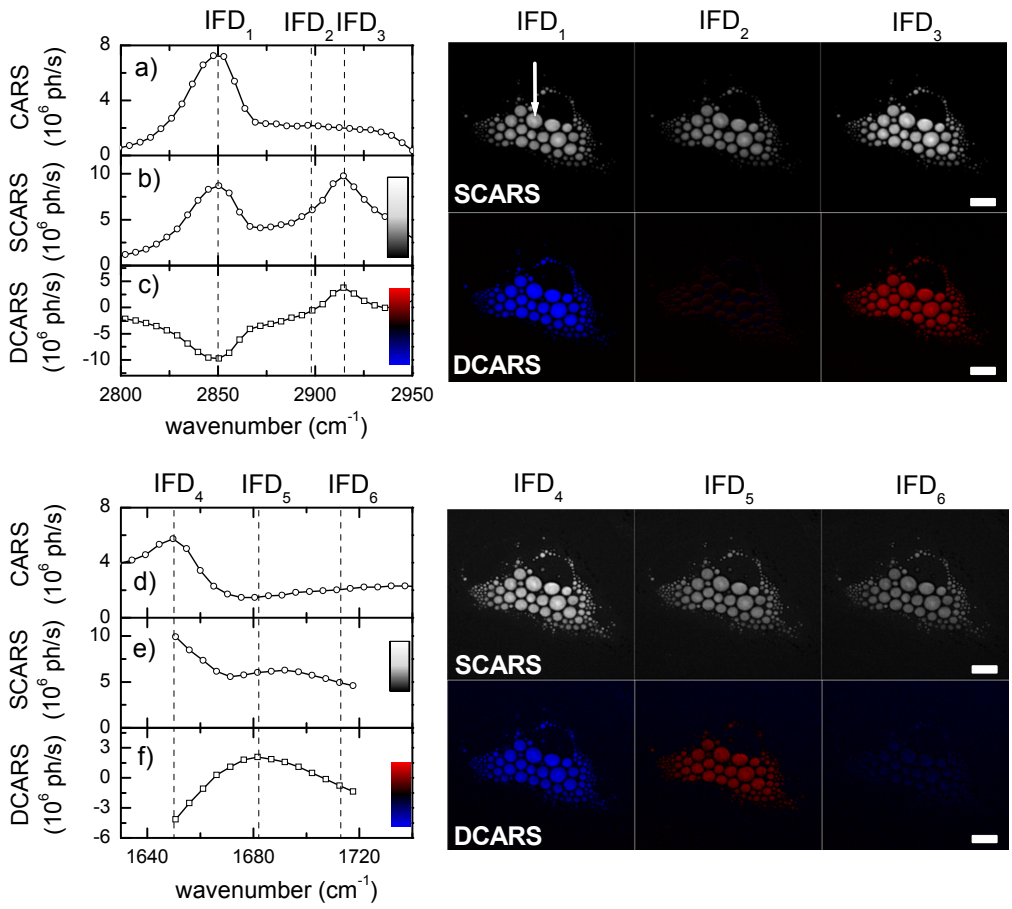

Fig. 6. CARS and D-CARS hyperspectral imaging of differentiated human adipose derived stem cells using the 60× 1.27 NA objective. Top left: CARS spectrum in the CH-stretch range of the lipid droplet indicated by the white arrow on the right using a single pulse pair Π_1 (a), and two pulse pairs Π_1 and Π_2 exciting two vibrational frequencies separated by 65 cm^{-1} giving rise to (b) the sum-CARS spectrum (SCARS) and (c) the difference CARS spectrum (DCARS). Top right: Extracts of sum-CARS and D-CARS *xy* images from the hyperspectral movie (Media 1 for D-CARS) at three instantaneous frequency differences IFD_1= 2850 cm^{-1}, IFD_2= 2898 cm^{-1}, IFD_3= 2915 cm^{-1} as indicated by the dashed lines in a). The grey and color scales are given in b), c) and refer to the y-axis. Power of pump 15 mW and Stokes 7 mW, 80 × 80 μm, 801 × 801 pixels, 0.01 ms pixel dwell time. Scale bars 10 μm. Bottom left: as top left but over the fingerprint spectral range and with Π_1 and Π_2 exciting two vibrational frequencies separated by 38 cm^{-1}. Bottom right: Extracts of sum-CARS and D-CARS *xy* images from the hyperspectral movie (Media 2 for D-CARS) at three instantaneous frequency differences IFD_4= 1650 cm^{-1}, IFD_5= 1682 cm^{-1}, IFD_6= 1713 cm^{-1}. Power of pump 22 mW and Stokes 10 mW.

of D-CARS to distinguish the chemical composition of micron-sized lipid droplets containing saturated or poly-unsaturated triglycerides [17], and have extended the technique to quadruplex CARS (Q-CARS) [15]. In the example shown in Fig. 6 the sign of the D-CARS contrasts correlates with the CARS spectral lineshapes obtained using a single pulse pair (Π_1), as expected. This is because D-CARS is given by CARS at Π_2 minus CARS at Π_1, where Π_2 excites

#181809 - $15.00 USD Received 14 Dec 2012; revised 1 Feb 2013; accepted 14 Feb 2013; published 13 Mar 2013

smaller IFDs, hence positive slopes appear as negative D-CARS contrasts [17]. Importantly, from the added lineshape information (hence chemical specificity) directly encoded in the sign of D-CARS, this technique can offer rapid imaging speed by discriminating chemical species at few wavenumbers with no need of lengthy spectral scans [17]. Moreover D-CARS rejects spectrally-constant non-resonant CARS contributions hence improves the signal-to-background ratio.

4. Conclusion

We have developed a multimodal hyperspectral CARS/TPF/SHG microscope platform using a single-broadband laser source. The 5 fs Ti:sapphire laser provides CARS vibrational excitation from 1200 cm^{-1} to 3780 cm^{-1}, covering the fingerprint region and the CH/OH stretch in one system (as opposed to the use of a dual apparatus [12]). The higher wavelength range of the laser ($>$ 910 nm) is used for TPE. Spectral focussing is used to equally chirp the pump and Stokes pulses to $>$ 1 ps providing a spectral resolution of 10 cm^{-1}, while a prism-based pulse compressor enables us to achieve 30 fs Fourier limited pulses at the sample for most efficient TPE. Improved chemical specificity and rejection of the non-resonant CARS background is provided by a differential CARS technique. Importantly no laser tuning is required, offering a hands-off system. These modalities were integrated into a standard inverted microscope with epi-fluorescence, DIC and darkfield imaging resulting in a versatile and user-friendly multi-modal microscope for cell imaging applications.

Acknowledgments

This work was funded by the UK BBSRC Research Council (grant n. BB/H006575/1). PB acknowledges the UK EPSRC Research Council for her Leadership fellowship award (grant n. EP/I005072/1). Mouse tail sections were obtained from Emma Dalton (Cardiff University) from tissue destined for disposal.

#181809 - $15.00 USD Received 14 Dec 2012; revised 1 Feb 2013; accepted 14 Feb 2013; published 13 Mar 2013